



HAL
open science

Passive Impact Location Estimation Using Piezoelectric Sensors

Daniel Guyomar, Mickaël Lallart, Thomas Monnier, X.-J. Wang, Lionel Petit

► **To cite this version:**

Daniel Guyomar, Mickaël Lallart, Thomas Monnier, X.-J. Wang, Lionel Petit. Passive Impact Location Estimation Using Piezoelectric Sensors. *Structural Health Monitoring*, 2009, 8 (5), pp.357-367. 10.1177/1475921709102090 . hal-00431380

HAL Id: hal-00431380

<https://hal.science/hal-00431380v1>

Submitted on 22 Mar 2023

HAL is a multi-disciplinary open access archive for the deposit and dissemination of scientific research documents, whether they are published or not. The documents may come from teaching and research institutions in France or abroad, or from public or private research centers.

L'archive ouverte pluridisciplinaire **HAL**, est destinée au dépôt et à la diffusion de documents scientifiques de niveau recherche, publiés ou non, émanant des établissements d'enseignement et de recherche français ou étrangers, des laboratoires publics ou privés.



Distributed under a Creative Commons Attribution - NonCommercial 4.0 International License

Passive Impact Location Estimation Using Piezoelectric Sensors

Daniel Guyomar, Mickaël Lallart,* Thomas Monnier,
Xingjun Wang and Lionel Petit

LGEF, INSA-Lyon, 8 rue de la Physique, F-69621, France

As part of Structural Health Monitoring (SHM), the history of a structure has become a crucial element to take into account. This has been shown, for example, by the spectacular accident of the flight Aloha 243 near Hawaiï, when a whole part of the fuselage of a Boeing 737 had been torn off. Thus, monitoring impacts has become particularly interesting to give a comprehensive view of the occurrence of structural damage. Typical impact location estimation techniques use structural frequency drifts of a structure. Thus, such methods need an external excitation of the structure, which is unrealistic in most of the cases. As well, huge and possibly long computations, as genetic algorithms or artificial neural networks, are required for such techniques in order to retrieve the impact location. The scope of this article was to present a passive impact location estimation using piezoelectric elements for a 1D infinite beam. The principles of the proposed technique was the comparison of the vibrational energy extracted by each sensor. From this comparison, the impact location was cost-efficiently estimated. Theoretical development and experimental results showed that this extraction-based force location estimation method performed well, while being very simple.

Keywords piezoelectric · passive detection · impact location estimation

1 Introduction

Having the knowledge of the history of a structure is as important as having an idea of its current condition in Structural Health Monitoring (SHM) systems. However, although SHM techniques have been extensively studied these last years, most of the researches focus on estimating the current status of a structure by periodical inspections rather than continuous monitoring. For example C-Scan or Lamb wave inspections can be regularly scheduled or can be done if a perceptible particular event arises, therefore disregarding the evolution and the

history of the structure that can give precious information about its health. However, some studies have been carried out on impact location estimation and/or tactile sensors, thus continuously monitoring the structure. These methods are either theoretical, with no experimental results [1], or rely on change of resonance frequency, necessitating high computational abilities and external excitation force, requiring external power supply [2–9]. This power supply requirements can compromise the possibility for the integration of embedded sensors (due to maintenance for example). Hence, a purely passive system that does not need any external power for supplying sensors

*Author to whom correspondence should be addressed.
E-mail: mickael.lallart@insa-lyon.fr

and/or actuators would therefore be greatly beneficial. Few studies, such as the work done by Thorp et al. [10], allow an efficient estimation of the wave propagation in the presence of shunted piezoelectric patches. However, this work focuses on wave transmission suppression, where the shunting capabilities of aperiodically spaced piezoelectric patches are used to confine the vibration near the excitation source.

Power flow in the structure can nevertheless give precious information that can be used for impact spatial location estimation. In this field, numerous studies have been carried out [11–13], but have not extended the work to location estimation.

The scope of this article is to propose a very simple way of location estimation, based on the power flow of the wave generated by an impact. The principle of the proposed technique is to compare the energy extracted by shunted piezoelectric inserts to estimate the location of the source of the wave. Only the energy from the wave created by the impact is needed for the estimation of the impact location, therefore no additional energy is required contrary to active methods. The article is organized as follows. Section 2 introduces the principles of the proposed method. Section 3 proposes a theoretical development based on the fundamental equation of motion and piezoelectric equations, in the case of an infinite lossless beam. This section also

includes an energetic analysis, as well as a performance discussion. Section 4 aims at validating the model by simulating the response of the sensors using a lumped model. In Section 5, experimental measurements are carried out to demonstrate the feasibility of the method, and to discuss the advantages and the drawbacks of the practical implementation. Finally, Section 6 concludes the article.

2 Principles

The proposed technique considers a 1D beam with resistively shunted piezoelectric elements bonded on the structure as shown Figure 1. Besides, the beam is considered as lossless and infinite. Considering an impact on the beam, the longitudinal waves generated by this force would travel in opposite direction along each part of the beam, as well as the energy flow. However, each time a wave goes through a piezoelectric insert, a part of its energy is converted into electrical energy that is dissipated through the resistor. Therefore, the wave energy decreases each time it passes a piezoelectric insert (Figure 2). Assuming that each shunted piezoelectric insert converts the same ratio of mechanical energy, an estimation of the source location can be given by comparing the energy that has been dissipated by the resistor.

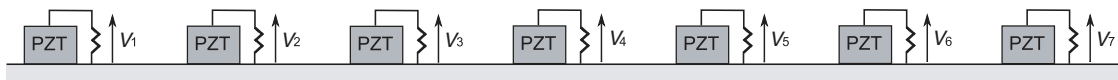


Figure 1 Example of PZT bonded beam.

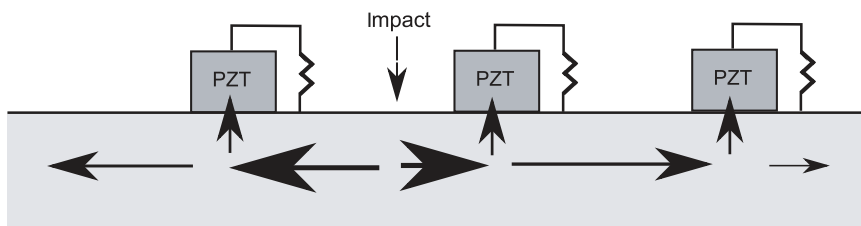


Figure 2 Energy flow in the beam.

3 Modeling

3.1 Propagation Model

The proposed structure is the infinite lossless beam (Figure 1) that supports dispersive Lamb waves. For the sake of clearness we use a crude modeling based on a nondispersive wave equation to describe the propagation in the beam. Such a model is simple and sufficient to enlighten the underlying principles of the technique.

In the case of purely mechanical parts (i.e., without piezoelectric inserts), the stress T and the strain S are directly proportionnal (1), with c the elastic constant. Applying Newton's law thus yields (2) in 1D, with m the lineic mass density and S_0 the cross-section of the beam. F represents a time finite force density, modeling the impact. For simplicity reasons, it will be considered in the followings that F is spatially limited to a part bounded by two piezoelements.

In the case of piezoelectric parts deriving 1D fundamental piezoelectric Equations (3) yields (4) by application of the Newton's law, and considering that no force density is applied on such parts. E is given as the electric field, D the induction field, e the voltage coefficient and ϵ^S the electric constant. ∇ is the Nabla operator and \bullet refers to the inner product.

$$T_{xx} = cS_{xx} = c \frac{\partial u(x, t)}{\partial x} \quad (1)$$

$$\begin{aligned} m \frac{\partial^2 u(x, t)}{\partial t^2} &= S_0 \nabla \cdot T + F(x, t) = S_0 \frac{\partial T_{xx}}{\partial x} + F(x, t) \\ &= cS_0 \frac{\partial^2 u(x, t)}{\partial x^2} + F(x, t) \end{aligned} \quad (2)$$

$$\begin{aligned} T_{xx} &= cS_{xx} - eE_z \\ D_z &= \epsilon^S E_z + eS_{xx} \end{aligned} \quad (3)$$

$$m \frac{\partial^2 u(x, t)}{\partial t^2} = cS_0 \frac{\partial^2 u(x, t)}{\partial x^2} - eS_0 \nabla \bullet E_z \quad (4)$$

From the second equation in (3) and considering Maxwell's equations for a purely dielectric material yields (5), with j the current density.

Thus connecting a resistor with a resistivity ρ to the piezoelement leads to (6) and the electric field is given as (7). Merging Equations (4) and (7) and considering that the time derivative of the strain evolves very slowly compared the time constant $\rho\epsilon$ thus yields $E_z \approx -\rho e \dot{S}_{xx}$, leading to the Stokes Equation (8). Therefore, the second right-hand side term can be seen as a local electromechanical damper, with a part of the energy dissipated into the resistor. The expression of the damping coefficient C_{eq} is given by (9).

$$j_z = -\dot{D}_z = -\epsilon^S \dot{E}_z - e \dot{S}_{xx} \quad (5)$$

$$E_z = -\rho e \dot{S}_{xx} - \rho \epsilon^S \dot{E}_z \quad (6)$$

$$E_z = -\frac{e}{\epsilon^S} \dot{S}_{xx} * e^{-\frac{t}{\rho\epsilon^S}} \quad (7)$$

$$m \frac{\partial^2 u(x, t)}{\partial t^2} = cS_0 \frac{\partial^2 u(x, t)}{\partial x^2} + \rho e^2 S_0 \frac{\partial^3 u(x, t)}{\partial x^2 \partial t} \quad (8)$$

$$C_{eq} = \rho e^2 S_0 \quad (9)$$

Resolving (2) for a monochromatic wave propagating along nonpiezoelectric parts leads to the trivial solution of the displacement (10). When the wave travels through piezoelectric parts and assuming negligible effects on the wave number yields (11) from (8). Consequently, noting U_n the magnitude of the displacement before a piezoelectric part and U_{n+1} the magnitude of the displacement after a piezoelectric part, and for a wave propagating in the direction of the increasing n yields (12), with l the length of a piezoelectric insert.

$$u(x, t) = A e^{\pm j(\omega t - \alpha x)} \quad \text{with} \quad \alpha = \omega \sqrt{\frac{m}{cS_0}} \quad (10)$$

$$\begin{aligned} u(x, t) &= A e^{\pm(j(\omega t - \alpha x) - \beta x)} \quad \text{with} \\ \beta &= \alpha \sqrt{\frac{(\rho e^2)^2 \omega^4}{c^2 + (\rho e^2 \omega)^2}} \end{aligned} \quad (11)$$

$$\frac{U_{n+1}}{U_n} = e^{-\beta l} \quad (12)$$

3.2 Energy Balance

The purpose of this section is to expose the dissipated energy over the two different parts of the system (i.e., purely mechanical and piezoelectric parts). It is considered that the propagating waves are included within the time period $[t_0; t_1]$ (i.e., $u(t, x) = \dot{u}(t, x) = \ddot{u}(t, x) = 0$ for $t < t_0$ and $t > t_1$). Besides, it is assumed that the Fubini's theorem can be applied.

The energy dissipated can be derived from the expression of the instantaneous field intensity vector given in (13), yielding the locally dissipated energy (14), where x_0 and $x_0 + L$ are the boundaries of the considered volume.

Considering (1), the energy balance for the 1D nonpiezoelectric parts yields (15). The time integration of the first term leads to a zero value for finite wave, and using (2) gives the total dissipated energy (16), which is zero for finite wave.

$$I = -\frac{\partial u}{\partial t} T \quad (13)$$

$$\begin{aligned} W &= \int_{x_0}^{x_0+L} \left(\int_{t_0}^{t_1} \left(-S_0 \nabla \bullet I + \frac{\partial u(x, t)}{\partial t} F \right) dt \right) dx \\ &= \int_{x_0}^{x_0+L} \left(\int_{t_0}^{t_1} \left(S_0 \frac{\partial^2 u(x, t)}{\partial t \partial x} T_{xx} + S_0 \frac{\partial u(x, t)}{\partial t} \frac{\partial T_{xx}}{\partial x} \right. \right. \\ &\quad \left. \left. + \frac{\partial u(x, t)}{\partial t} F \right) dt \right) dx \end{aligned} \quad (14)$$

$$\begin{aligned} W_m &= \int_{x_0}^{x_0+L} \left(\int_{t_0}^{t_1} \left(\frac{S_0}{c} \dot{T}_{xx} T_{xx} + \frac{\partial u(x, t)}{\partial t} \right. \right. \\ &\quad \left. \left. \times \left(S_0 \frac{\partial T_{xx}}{\partial x} + F \right) \right) dt \right) dx \end{aligned} \quad (15)$$

$$W_m = m \int_{x_0}^{x_0+L} \left(\int_{t_0}^{t_1} \dot{u}(x, t) \ddot{u}(x, t) dt \right) dx = 0 \quad (16)$$

A similar development shows that the energy dissipated over the piezoelectric parts is given by (17) from (2) and (3), and considering constant electrical field over the x -axis, with R the shunt resistor and V the voltage of the piezoelement. This energy can also be calculated using Fubini's and Green-Ostrogradski's theorems yielding (18). As previously seen, only the damping part intervenes in the energy balance, thus giving (19).

Considering monochromatic waves as (11) so leads to (20).

$$\begin{aligned} W_p &= eS_0 \int_{x_0}^{x_0+L} \left(\int_{t_0}^{t_1} \left(\frac{\partial^2 u}{\partial x \partial t} E_z \right) dt \right) dx \\ &= -\frac{S_0}{\rho} \int_{x_0}^{x_0+L} \left(\int_{t_0}^{t_1} E_z^2 dt \right) dx \\ &= -\frac{S_0}{\rho l} \int_{t_0}^{t_1} V^2 dt = -\frac{1}{R} \int_{t_0}^{t_1} V^2 dt \end{aligned} \quad (17)$$

$$W_p = S_0 \int_{t_0}^{t_1} (I(x_0 + l) - I(x_0)) dt \quad (18)$$

$$\begin{aligned} W_p &= C_{eq} \int_{t_0}^{t_1} \left(\frac{\partial^2 \dot{u}(x_0 + l, t)}{\partial x^2} \dot{u}(x_0 + l, t) \right. \\ &\quad \left. - \frac{\partial^2 \dot{u}(x_0, t)}{\partial x^2} \dot{u}(x_0, t) \right) dt \end{aligned} \quad (19)$$

$$W_p = C_{eq} (1 - e^{-2\beta l}) \int_{t_0}^{t_1} \left(\frac{\partial^2 \dot{u}(x_0, t)}{\partial x^2} \dot{u}(x_0, t) \right) dt \quad (20)$$

Considering that x_0 is the spatial origin of the wave gives (21), where W_0 is the source wave energy and W_{p0} the nearest piezoelectric elements (one for each direction). Thus considering the n^{th} piezoelement (starting from the wave source) yields a remaining energy (22) and leads to (23). Consequently, comparing the extracted energy values through the use of (17) it is possible to determine the source of the wave (i.e., the location of the impact). In order to have a more robust estimation of the impact location, the criterion (24) is proposed. The location estimation of the wave source can be done by determining the zero crossing of this criterion. This is explained by the fact that the first two shunted patches absorb more energy than the other patches. Therefore, from the origin of the wave, the energy dissipated through the shunt resistor is a decreasing value of the distance from the patch to the energy source. Therefore, the criterion (24) that performs a differentiation of the dissipated energy is null considering the two shunted patches that are closest to the source. Then, the energy being a decreasing function of the distance from the source (as each patch absorbs a part of the mechanical energy of the wave), the criterion reaches a minimal and a maximal value for the next set of patches, and then decreases in

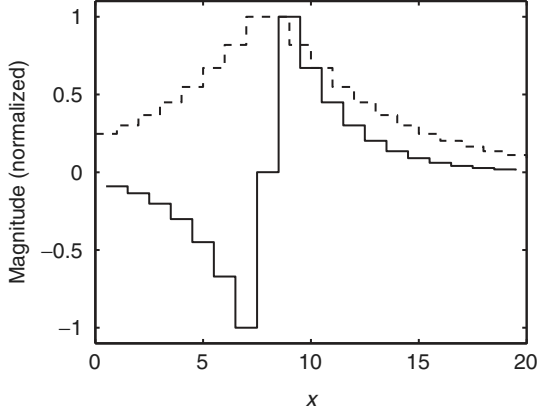


Figure 3 Normalized evolutions of the extracted energy (dotted) and the proposed criterion (plain) for a wave propagating from $x_0 = 7.5$ and $\beta l = 0.1$.

absolute value. The signum of the criterion depends both on the wave direction and the direction the estimation is performed. If the wave and criterion directions are the same (*resp.* opposite), then the criterion is positive (*resp.* negative). Consequently for a wave incoming from the left the criterion would be positive, and negative for a wave incoming from the right. Figure 3 shows the evolution of the extracted energy and the criterion for a wave propagating from the point $x_0 = 7.5$. The patches are assumed to be placed at integer values of x . As expected, the criterion is null near impact location, then reaches a minimal and maximal values, and starts decreasing in absolute value, with a signum depending on the wave direction and criterion direction.

$$W_{p_0} = (1 - e^{-2\beta l}) W_0 \quad (21)$$

$$W_{n+1} = e^{-2\beta l} W_n \quad (22)$$

$$\begin{aligned} W_{p_n} &= (1 - e^{-2\beta l}) W_{n-1} \\ &= (1 - e^{-2\beta l}) e^{-2n\beta l} W_0 \end{aligned} \quad (23)$$

$$W_{p_n} - W_{p_{n-1}} = \frac{1}{R} \int_{t_0}^{t_1} (V_n(t)^2 - V_{n-1}(t)^2) dt \quad (24)$$

3.3 Performance Discussion

As the impact location estimation accuracy is given by the inter-piezo length, this method is not so precise compared to standard methods, but is much faster and computationally efficient. It is

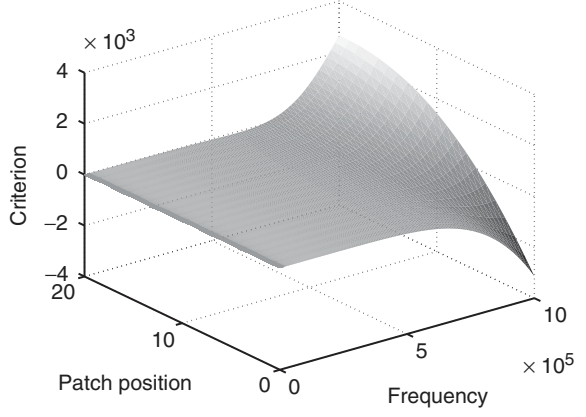


Figure 4 Evolution of the criterion as a function of the frequency.

also believed that, as the detection is based on energy flow, the noise influence is quite limited. Besides, its main advantage lies on the passive nature of the detection. Indeed, there is no need of external power supply to the sensors, and there is absolutely no need of exciting the beam with a predefined source. As well, taking into account the structural damping of the beam would probably allow a better detection by interpolation. This last observation is nevertheless out of the scope of this article. Finally, as shown in the experimental results, taking into account drifts in the coupling coefficient (introduced by the bonding) is very easy, by adjustment of the resistance value in order to equalize the energy extraction ratio for each piezoelectric insert.

Figure 4 depicts the evolution of the criterion as a function of the wave frequency (parameters are those taken in the next section), which shows that the criterion signum is constant over the frequency for a given patch position. Therefore, considering that there is no mode conversion, the estimation of the impact location can also be performed in a correct manner with multichromatic waves. Moreover, this figure shows that the proposed criterion is more sensitive to high frequencies.

4 Simulated Response

Simulations using numerical integration have been carried out in order to confirm the model.

The beam is modeled by spring-mass systems localized on each node. In addition, some nodes include piezoelectric elements connected to a resistor and modeled by basic Equations (3). Simulation parameters are given Table 1. The piezoelectric coefficients are taken from the literature and correspond to NAVY-III type of piezoelectric elements.

Simulation results are shown in Figure 5 considering a tone-burst excitation at 500 kHz

Table 1 Simulation parameters (ϵ_0 is taken as the vacuum dielectric constant).

<i>Beam parameters</i>	<i>Piezoelectric parameters</i>	<i>Other parameters</i>
S_0	12.10^{-5} m^2	1 3 mm ω $1000.10^3 \pi \text{ rad s}^{-1}$
m	210 g.m^{-1}	ϵ^S $1142.\epsilon_0$ R 15Ω
c	14.6 GPa	e -6.18 C m^{-1}

and in Figure 5 considering a Gaussian force input with a frequency band of 500 kHz. The value of βl derived from (11) is 0.1618. The dots represent nodes including piezoelectric patches. As expected, the source of the wave (i.e., the impact location) is quite well estimated by the zero crossing of the criterion, although some points are not exactly on the theoretical curve. This could be explained by the finite time integration performed during the simulation and simulation accuracy (as a trade-off between space and time accuracy appears). Therefore, when the source is out of the scanning range (e.g., nodes 150 and 253), the criterion is monotonous with a signum given by the direction the criterion is performed and the source location. When the impact source is within the scanning range, the criterion crosses the zero value in the impact area, and then reaches an extremum and decreases in absolute value, with the signum

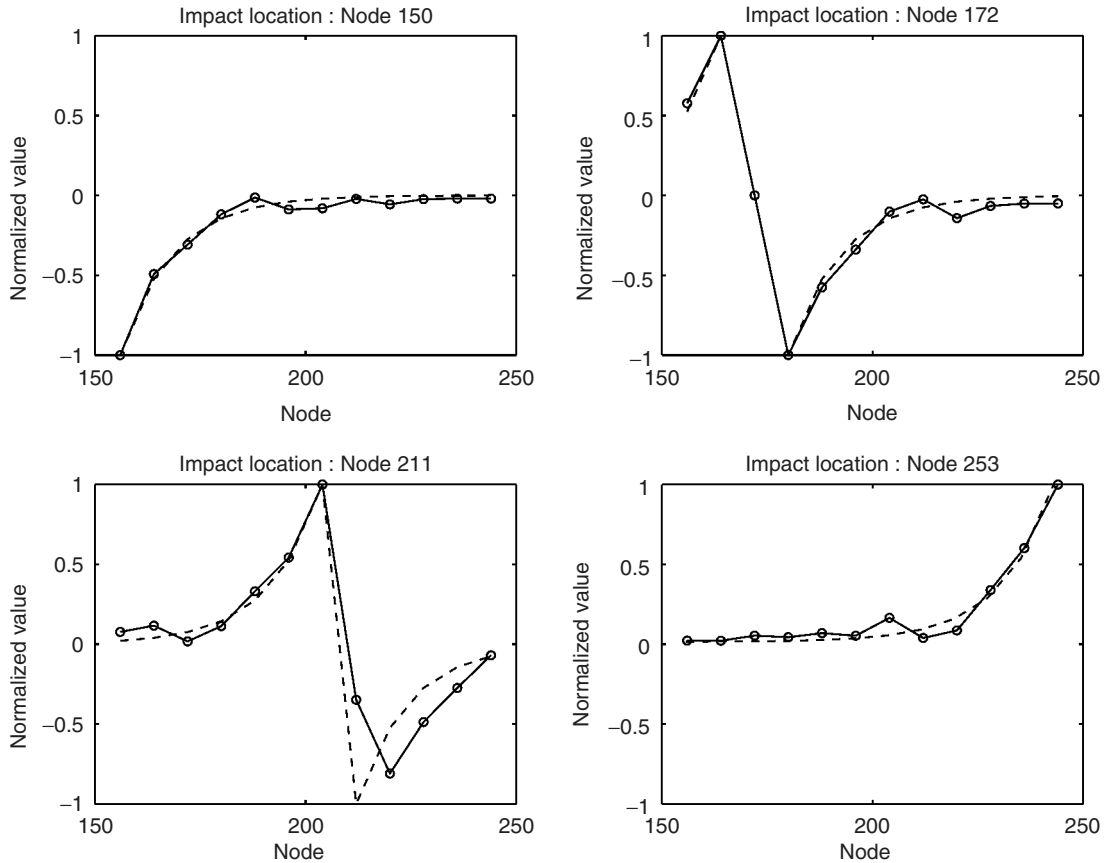


Figure 5 Simulated (plain) and theoretical (dotted) results for the proposed criterion using a sine tone burst.

depending on the criterion and energy flow directions (Figure 6).

5 Experimental Results

5.1 Experimental Set-up

In order to confirm the effectiveness of the proposed method, experimental measurements were done considering a $350 \times 50 \times 3 \text{ mm}^3$ Bulk Molding Compound (BMC) beam as shown Figure 7. Seven resistively shunted piezoelectric inserts (Q&SP1-89 ceramic) with dimensions of

$30 \times 3 \times 0.5 \text{ mm}^3$ and each separated by a distance of 40 mm are bonded onto the upper surface of the beam. As the coupling of each piezoelectric insert is different due to the variability of the bonding conditions, the value of each resistor has been tuned in order to have the same ratio of extracted energy for each piezoelectric patch. Moreover, in order to preserve the infinite beam assumption, dampers have been added at each end of the beam. The parameters are consigned in Table 1, except for the value of the resistance, which is tuned to equalize the energy extraction ratio due to the bonding.

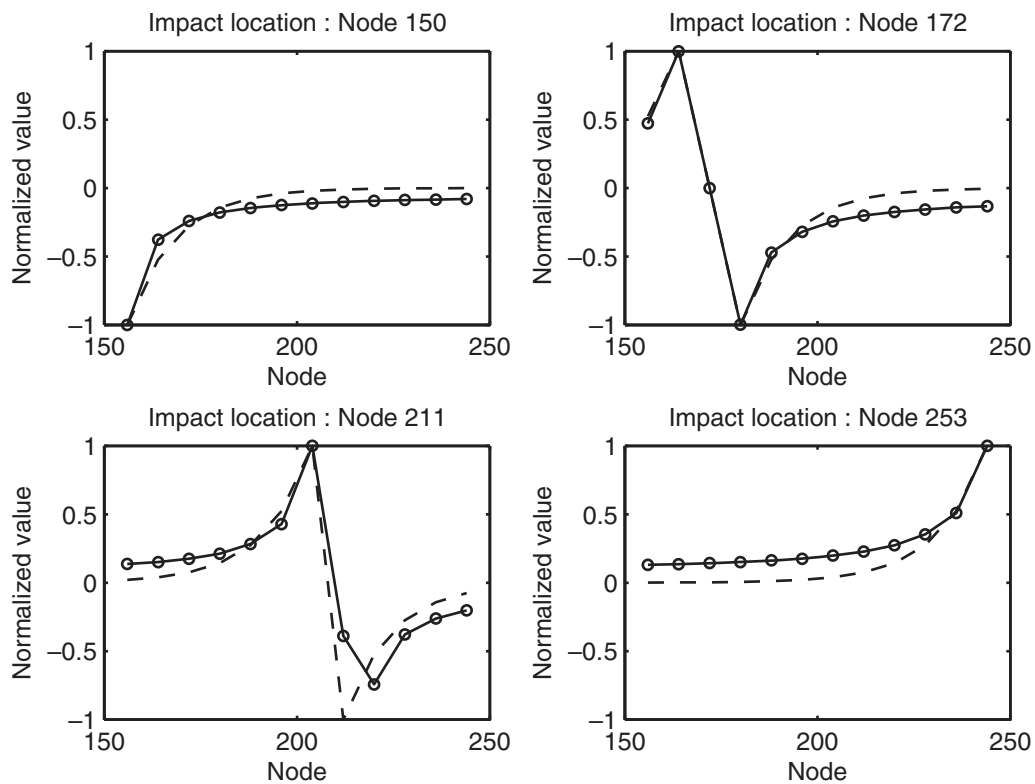


Figure 6 Simulated (plain) and theoretical (dotted) results for the proposed criterion using Gaussian force waveform.

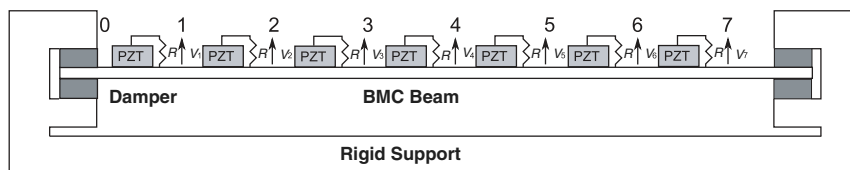


Figure 7 Experimental set-up.

5.2 Results and Discussion

In a first approach the source is a moveable piezoelectric patch that is excited by a sine burst of 10 periods at a frequency of 530 kHz (for repeatability reasons), corresponding to its first flexural mode. Experimental results are shown Figure 8. Due to the drifts in the bonding, the value of βl is extrapolated from the measurements, giving $\beta l = 0.4$. Results show that the impact location is quite well estimated by the zero crossing of the criterion, and follows theoretical predictions in a similar fashion, with a response depending on criterion and wave directions. Furthermore, the internal damping coefficient, although being very small, gives an exact idea of the impact location (in this case exactly in the middle), as in this case the energy flow also decreases in nonpiezoelectric parts. The differences

with the theoretical curve are explained by the lossless and infinite beam assumptions, as well as the broadband and dispersive nature of the waves.

A second set of measurements consists in impacting the beam with an impulse hammer in order to mimic low-velocity impacts. Indeed, this kind of pulse excitation is far more representative of the kind of impact that the structure to be monitored is likely to endeavor during its service. Hence, the multi-frequency stress waves induced by the hammer impact produce much more broadband ultrasonic signatures. Figure 9 showing the resulting waveforms of the applied force as well as the voltage of two patched (3 and 4) when impacting the beam in position 4 illustrates this multi-frequency properties of the traveling waves.

Comparison between experimentally extracted values of the proposed criterion and theoretically

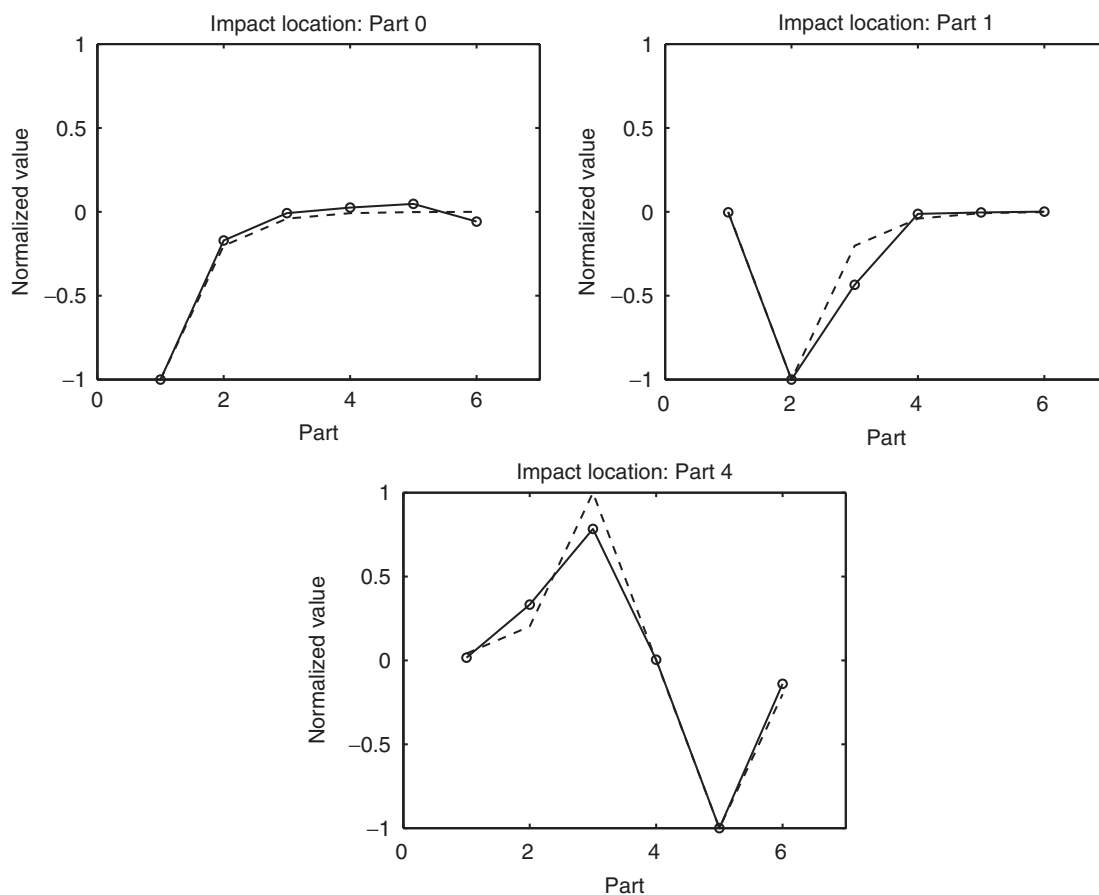


Figure 8 Experimental (plain) and theoretical (dotted – interpolated value of βl) results for the proposed criterion using a – 530 kHz piezoelectric moveable source.

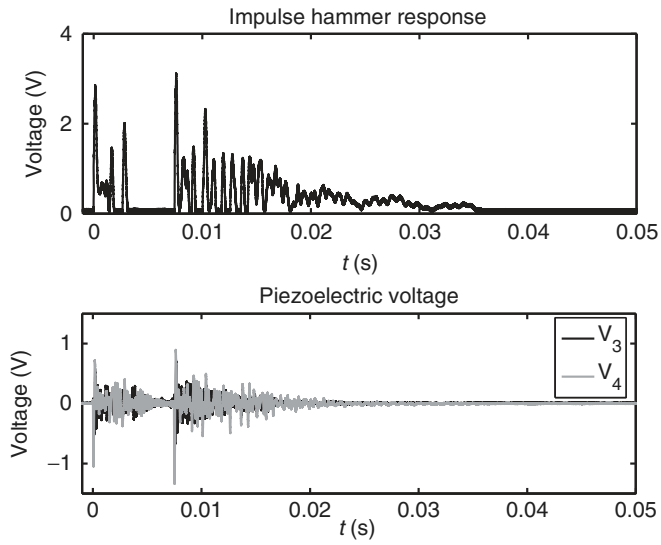


Figure 9 Example of the impulse hammer response (top) and patches 3 and 4 (bottom) when impacting the beam in position 4.

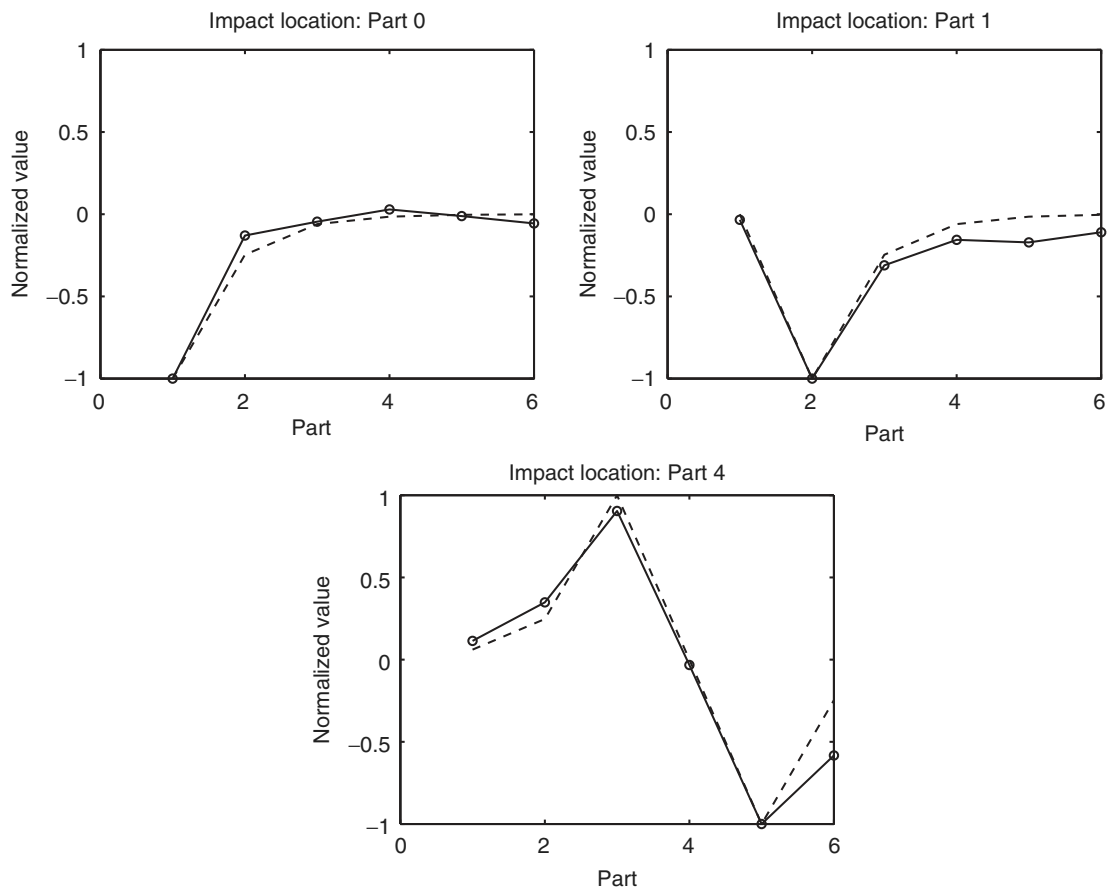


Figure 10 Experimental (plain) and theoretical (dotted – interpolated value of βl) results for the proposed criterion using an impact hammer.

predicted ones are shown in Figure 10. The value of βl is set to 1.4. As previously described, these results show a good agreement with theoretical predictions, allowing to accurately estimate the impact location. The proposed energy-based criterion is, therefore, a well-adapted impact location estimator. Taking into account the structural damping may also give a better estimation of the impact location. The slight differences between theoretically predicted and experimentally measured criteria can be explained by the dispersive behavior and spatial filtering of the traveling waves.

6 Conclusion and Future Work

Impact location estimation and monitoring can give precious information on the evolution of the health of a structure. However classical methods of location estimation and/or tactile sensing make the practical implementation quite uneasy. This article proposed a simple way of impact location estimation based on resistively shunted piezoelectric inserts. The principles of the method rely on the comparison of the extracted electrical energy by each sensor. These piezoelectric elements can be seen as local electro-mechanical dampers that give insight of the energy flow. Thus comparing the extracted energy of each piezoelectric elements leads to a simple and quite efficient impact location estimation.

This study considers infinite lossless beam, as well as resistive shunt. Future work considering a lossy finite beam would lead to a more realistic model, and therefore to a finer impact location estimation. Besides, it is believed that taking into account internal losses in the beam can predict more accurately the impact location by extrapolation. In addition to resistive shunts, inductive or nonlinear shunts have to be investigated. Also, the question of the location of multiple impacts has not been investigated in the present contribution. Indeed, simultaneous impacts would lead to interferences of waves from several forces locations, with possible cancelation of the energy at

the location of a piezoelectric element. Further investigation will consist in assessing the capability of the proposed method not to miss the detection and to locate the impacts in this context. Finally, the extension of the method to 2D structures like plates is also a very interesting field of investigation.

References

1. Romano, A.J., Abraham, P.B. and Williams, E.G. (1990). A poynting vector formulation for thin shells and plates, and its application to structural intensity analysis and source localisation. Part I: theory, *Journal of the Acoustical Society of America*, 87(3), 1166–1175.
2. Ping, L. and Yumei, W. (1996). An arbitrarily distributed tactile sensor array using piezoelectric resonator, In: *IEEE Instrumentation and Measurement Technology Conference*, Brussels, Belgium.
3. Maezawa, M., Imahashi, T., Kuroda, Y., Adachi, H. and Yanagisawa, K. (1997). Tactile sensor using piezoelectric resonator, In: *1997 International Conference on Solid-State Sensors and Actuators*, Chicago.
4. Seydel, R. and Chang, F. K. (2001). Impact identification of stiffened composite panels: I. system development, *Smart Materials and Structures*, 10(2), 354–369.
5. Seydel, R. and Chang, F.K. (2001). Impact identification of stiffened composite panels: II. Implementation studies, *Smart Materials and Structures*, 10(2), 370–379.
6. Peelamedu, S.M., Ciocanel, C. and Naganathan, N.G. (2004). Impact detection for smart automotive damage mitigation systems, *Smart Materials and Structures*, 13(5), 990–997.
7. Murali Krishna, G. and Rajanna, K. (2004). Tactile sensor based on piezoelectric resonance, *IEEE Sensors Journal*, 4(5), 691–697.
8. Hu, N., Fukunaga, H., Matsumoto, S., Yan, B. and Peng, X.H. (2007). An efficient approach for identifying impact force using embedded piezoelectric sensors, *International Journal of Impact Engineering*, 34(7), 1258–1271.
9. Lee, M.L., Chiu, W.K., and Koss, L.L. (2005). Numerical study into the reconstruction of impact forces on railway track-like structures, *International Journal of Impact Engineering*, 34(7), 1258–1271. *Structural Health Monitoring*, 4(1), 19–45.

10. Thorp, O., Ruzzene, M. and Baz, A. (2001). Attenuation and localization of wave propagation in rods with periodic shunted piezoelectric patches, *Smart Materials and Structures*, 10(5), 979–989.
11. Noiseux, D. U. (1970). Measurement of power flow in uniform beams and plates, *Journal of the Acoustical Society of America*, 47(1B), 238–247.
12. Liu, Y., Wang, C.-H. and Ying, C.-F. (1991). Transient waves in a piezoelectric half-space generated by line-loaded surface sources, In: *Proceedings of the IEEE Ultrasonics Symposium*, 1, 377–381.
13. Audrain, P., Masson, P. and Berry, A. (2000). Investigation of active structural intensity control in finite beams: theory and experiment, *Journal of the Acoustical Society of America*, 108(2), 612–623.